Tradeoffs between microbial growth phases lead to frequency-dependent and non-transitive selection

Michael Manhart, Bharat V. Adkar, and Eugene I. Shakhnovich*
Department of Chemistry and Chemical Biology,
Harvard University, Cambridge, MA 02138, USA
(Dated: November 2, 2017)

Mutations in a microbial population can improve the frequency of a genotype not only by increasing its exponential growth rate, but also by decreasing the lag time or adjusting the yield (resource efficiency). The contribution of multiple life-history traits to selection is a critical question for evolutionary biology as we seek to predict the evolutionary fates of mutations. Here we use a model of microbial growth to show there are two distinct components of selection corresponding to the growth and lag phases, while the yield modulates their relative importance. The model predicts nontrivial population dynamics when there are tradeoffs between phases: multiple strains can coexist over long times due to frequency-dependent selection, and strains can engage in rock-paper-scissors interactions due to non-transitive selection. We characterize the environmental conditions and patterns of traits necessary to realize these phenomena, which we show to be readily accessible to experiments. Our results provide a theoretical framework for analyzing high-throughput measurements of microbial growth traits, especially interpreting the pleiotropy and correlations between traits across mutants. This work also highlights the need for more comprehensive measurements of selection in simple microbial systems, where the concept of an ordinary fitness landscape breaks down.

Keywords: microbial growth; frequency-dependent selection; coexistence; non-transitive selection

I. INTRODUCTION

The life history of most organisms is described by multiple traits, such as fecundity, generation time, resource efficiency, and survival probability [1]. While all of these traits may determine the long-term fate of a lineage, it is often not obvious how selection optimizes all of them simultaneously, especially if there are tradeoffs [2, 3]. The comparatively simple life histories of single-celled microbes make them a convenient system to study this problem. Microbial cells typically undergo a lag phase while adjusting to a new environment, followed by a phase of exponential growth, and finally a saturation or stationary phase when resources are depleted. Covariation in traits for these phases appears to be pervasive in microbial populations. Experimental evolution of *E. coli* produced wide variation of growth traits both between and within populations [4, 5], while naturally-evolved populations of yeast have environment-dependent patterns of covariation [6]. Covariation in growth traits appears to also be important in populations adapting to antibiotics [7–10]. Even single mutations have been found to be pleiotropic, generating variation in multiple phases [7, 11].

Previous work has focused mainly on the possibility of tradeoffs between these traits, especially between exponential growth rate and yield (resource efficiency) in the context of r/K selection [5, 7, 12–17], as well as between growth rates at low and high concentrations of a resource [18–21]. However, new methods for high-throughput phenotyping of microbial populations have recently been developed to generate large data sets of growth traits [22], measuring growth rates, lag times, and yields for hundreds or thousands of strains across environmental conditions [6]. Some methods can even measure these traits for populations starting from single cells [23, 24]. This data requires a quantitative framework to interpret observed patterns of covariation in an evolutionary context. For example, while growth tradeoffs have previously been proposed to cause coexistence of multiple strains [19, 21], we lack a quantitative understanding of what patterns of traits and conditions are necessary to achieve these effects, such that they can be directly evaluated on high-throughput data.

Here we develop a quantitative framework for selection on multiple microbial growth traits to address this problem. We derive an expression for the selection coefficient that quantifies the relative selection pressures on lag time, growth rate, and yield. We then determine how these selection pressures shape population dynamics over many cycles of growth, as occur in natural environments or laboratory evolution. We find that selection is frequency-dependent, enabling coexistence of multiple strains and swaying the fixation statistics of mutants from the classical expectation. We also find that selection can be non-transitive across multiple strains, leading to rock-paper-scissors interactions. These results are not only valuable for interpreting measurements of microbial selection and growth traits, but they also reveal how simple properties of microbial growth lead to complex population dynamics.

* To whom correspondence should be addressed. Email: shakhnovich@chemistry.harvard.edu

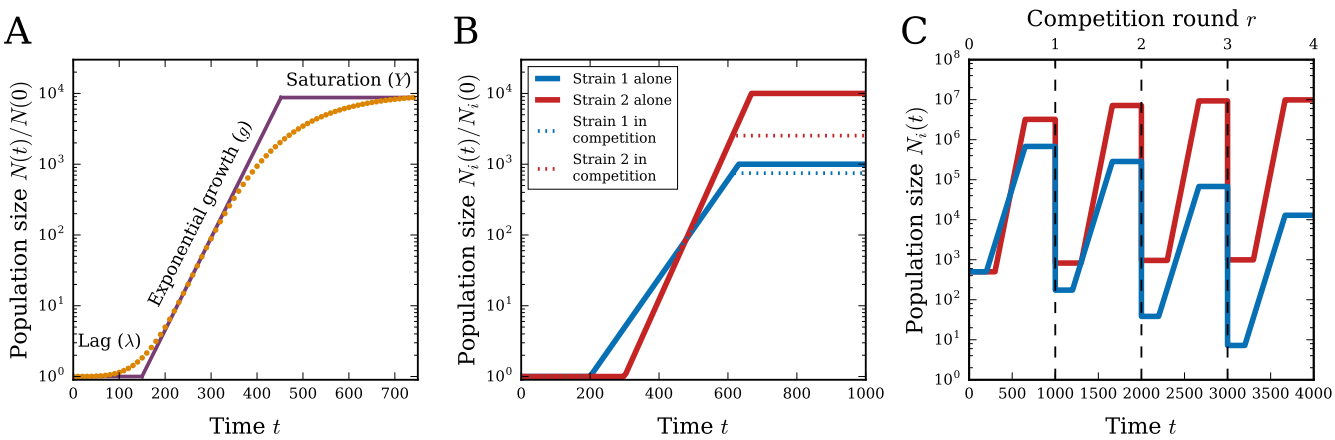

FIG. 1. Growth and selection in a microbial population. (A) Example growth curve (orange points) and the minimal three-phase model (solid violet line); each phase is labeled with its corresponding growth trait. (B) Two example growth curves in the three-phase model. Solid lines show the growth curves for each strain growing alone, while dashed lines show the growth curves of the two strains mixed together and competing for the same resources. Note that the solid and dashed growth curves are identical until saturation, since the only effect of competition is to change the saturation time. (C) Example growth curves over multiple rounds of competition. Each vertical dashed line marks the beginning of a new growth cycle, starting from the same initial population size and amount of resources.

II. METHODS

Consider a population of microbial cells competing for a single limiting resource. The population size $N(t)$ as a function of time (growth curve) typically follows a sigmoidal shape on a logarithmic scale, with an initial lag phase of sub-exponential growth, then a phase of exponential growth, and finally a saturation phase as the environmental resources are exhausted (Fig. 1A). We consider a minimal three-phase model of growth dynamics in which the growth curve is characterized by three quantitative traits, one corresponding to each phase of growth [25, 26]: a lag time λ, an exponential growth rate g, and a saturation population size N_{sat} (Supplementary Methods, Fig. 1A). It is possible to generalize this model for additional phases, such as a phase for consuming a secondary resource (diauxie) or a death phase, but here we will focus on these three traits since they are most commonly reported in microbial phenotyping experiments [6, 22].

The saturation size N_{sat} depends on both the total amount of resources in the environment, as well as the cells' intrinsic efficiency of using those resources. To separate these two components, we define R to be the initial amount of the limiting resource and Y to be the yield, or the number of cells per unit resource [4]. Therefore $N(t)/Y$ is the amount of resources consumed by time t, and saturation occurs at time t_{sat} when $N(t_{\text{sat}}) = N_{\text{sat}} = RY$. The saturation time t_{sat} is therefore determined intrinsically, e.g., by the growth traits of the strain, rather than being externally imposed. It is straightforward to extend this model to multiple strains with distinct traits g_i, λ_i, and Y_i, all competing for the same pool of resources (Supplementary Methods, Fig. 1B). We assume different strains interact only by competing for the limiting resource; their growth traits are the same as when they grow independently.

We focus on the case of two competing strains, such as a wild-type and a mutant. We will denote the wild-type growth traits by g_1, λ_1, Y_1 and the mutant traits by g_2, λ_2, Y_2. Assume the total initial population size is N_0 and the initial fraction of mutants is x. For simplicity we reduce the parameter space by using the following dimensionless quantities:

$$\begin{aligned} \text{Relative mutant growth rate:} \quad & \gamma = (g_2 - g_1)/g_1, \\ \text{Relative mutant lag time:} \quad & \omega = (\lambda_2 - \lambda_1)g_1, \\ \text{Relative wild-type yield:} \quad & \nu_1 = RY_1/N_0, \\ \text{Relative mutant yield:} \quad & \nu_2 = RY_2/N_0. \end{aligned} \tag{1}$$

Each relative yield is the fold-increase of that strain if it grows alone, starting at population size N_0 and with R resources.

Laboratory evolution experiments, as well as seasonal natural environments, typically involve a series of these growth cycles as new resources periodically become available [27]. We assume each round of competition begins with the same initial population size N_0 and amount of resources R, and the strains grow according to the dynamics of Fig. 1B until those resources are exhausted. The population is then diluted down to N_0 again with R new resources, and the cycle repeats (Fig. 1C). The total selection coefficient for the mutant, relative to the wild-type, for each round is [28, 29]

$$s = \log\left(\frac{N_2(t_{\text{sat}})}{N_1(t_{\text{sat}})}\right) - \log\left(\frac{N_2(0)}{N_1(0)}\right), \tag{2}$$

where time t is measured from the beginning of the round. This definition is convenient because it describes the relative change in frequency of the mutant over the wild-type during each round of competition. Let $x(r)$ be the mutant frequency at the beginning of the rth round of competition; the frequency at the end of the round will be the initial frequency $x(r+1)$ for the next round. Using Eq. 2, the selection coefficient for this round is $s(x(r)) = \log(x(r+1)/[1-x(r+1)]) - \log(x(r)/[1-x(r)])$, which we can rearrange to obtain

$$x(r+1) = \frac{x(r)e^{s(x(r))}}{1 - x(r) + x(r)e^{s(x(r))}}. \tag{3}$$

This shows how the mutant frequency changes over rounds as a function of the selection coefficient. If the selection coefficient is small, we can approximate these dynamics over a large number of rounds by the logistic equation: $dx/dr \approx s(x)x(1-x)$.

III. RESULTS

A. Distinct components of selection on growth and lag phases

We can derive an approximate expression for the selection coefficient as a function of the underlying parameters in the three-phase growth model. The selection coefficient consists of two components, one corresponding to selection on growth rate and another corresponding to selection on lag time (Supplementary Methods, Fig. S1):

$$s \approx s_{\text{growth}} + s_{\text{lag}}, \tag{4a}$$

where

$$\begin{aligned} s_{\text{growth}} &= A\gamma \log\left[\frac{1}{2}H\left(\frac{\nu_1}{1-x}, \frac{\nu_2}{x}\right)\right], \\ s_{\text{lag}} &= -A\omega(1+\gamma), \\ A &= \frac{(1-x)/\nu_1 + x/\nu_2}{(1-x)/\nu_1 + (1+\gamma)x/\nu_2}, \end{aligned} \tag{4b}$$

and $H(a,b) = 2/(a^{-1}+b^{-1})$ denotes the harmonic mean. The harmonic mean of the two yields is approximately the effective yield for the whole population (Supplementary Methods).

We interpret the two terms of the selection coefficient as selection on growth and selection on lag since s_{growth} is zero if and only if the growth rates are equal, while s_{lag} is zero if and only if the lag times are equal. In the limit of small relative differences in growth rate γ and lag time ω, these components of selection are

$$\begin{aligned} s_{\text{growth}} &\approx \gamma \log\left[\frac{1}{2}H\left(\frac{\nu_1}{1-x}, \frac{\nu_2}{x}\right)\right], \\ s_{\text{lag}} &\approx -\omega. \end{aligned} \tag{5}$$

As expected, s_{growth} is proportional to the ordinary growth rate selection coefficient $\gamma = (g_2 - g_1)/g_1$, while $-\omega = -(\lambda_2 - \lambda_1)g_1$ is the approximate selection coefficient for lag. This contrasts with previous studies that used $\lambda\, ds/d\lambda$ as a measure of selection on lag time [4, 30], which assumes that selection acts on the change in lag time relative to the absolute magnitude of lag time, $(\lambda_2 - \lambda_1)/\lambda_1$. But the absolute magnitude of lag time cannot matter since the model is invariant under translations in time, and hence our model correctly shows that selection instead acts on the change in lag time relative to the growth rate.

B. Effect of pleiotropy and tradeoffs on selection

Many mutations affect multiple growth traits simultaneously, i.e., they are pleiotropic [7, 11]. In particular, if a mutation affects both growth and lag, then both s_{growth} and s_{lag} will be nonzero. The ratio of these components indicates the relative selection on growth versus lag traits:

$$\frac{s_{\text{growth}}}{s_{\text{lag}}} = -\frac{\gamma}{\omega(1+\gamma)} \log\left[\frac{1}{2}H\left(\frac{\nu_1}{1-x}, \frac{\nu_2}{x}\right)\right]. \tag{6}$$

We can use this to determine, for example, how much faster a strain must grow to compensate for a longer lag time. This also shows that we can increase the magnitude of relative selection on growth versus lag by increasing the relative yields ν_1, ν_2. Conceptually, this is because increasing the yields increases the portion of the total competition time occupied by the exponential growth phase compared to the lag phase. Since each relative yield ν_i is proportional to the initial amount of resources per cell R/N_0, we can therefore tune the relative selection on growth versus lag in a competition experiment by controlling R/N_0. One can use this, for example, in an evolution experiment to direct selection more toward improving growth rate or more toward improving lag time.

The ratio $s_{\text{growth}}/s_{\text{lag}}$ also indicates the type of pleiotropy on growth and lag through its sign. If $s_{\text{growth}}/s_{\text{lag}} > 0$, then the pleiotropy is synergistic: the mutation is either beneficial to both growth and lag, or deleterious to both. If $s_{\text{growth}}/s_{\text{lag}} < 0$, then the pleiotropy is antagonistic: the mutant is better in one trait and worse in the other. Antagonistic pleiotropy means the mutant has a tradeoff between growth and lag. In this case, whether the mutation is overall beneficial or

deleterious depends on which trait has stronger selection. Since relative selection strength is controlled by the initial resources per cell R/N_0 through the yields (Eq. 6), we can therefore qualitatively change the outcome of a competition with a growth-lag tradeoff by tuning R/N_0 to be above or below a critical value, obtained by setting $s_{\text{growth}} = s_{\text{lag}}$:

$$\text{Critical value of } \frac{R}{N_0} = \frac{2e^{\omega(1+1/\gamma)}}{H\left(\frac{Y_1}{1-x}, \frac{Y_2}{x}\right)}. \tag{7}$$

The right side of this equation depends only on intrinsic properties of the strains (growth rates, lag times, yields) and sets the critical value for R/N_0, which we can control experimentally. When R/N_0 is below this threshold, selection will favor the strain with the better lag time: there are relatively few resources, and so it is more important to start growing first. On the other hand, when R/N_0 is above the critical value, selection will favor the strain with the better growth rate: there are relatively abundant resources, and so it is more important to grow faster.

Mutational effects on growth traits may not only be pleiotropic, but they may also be correlated. The simplest case is a linear correlation between growth traits across many mutations or strains:

$$\lambda \approx \frac{a}{g} + \text{constant}, \qquad \nu \approx bg + \text{constant}, \tag{8}$$

where a and b are proportionality constants. We take lag time to be linearly correlated with growth time (reciprocal growth rate), rather than growth rate, since then both traits have units of time and the constant a is dimensionless. Various models predict linear correlations of this form [31–36], which have been tested on measured distributions of traits [5–7, 15–17, 35] (see Discussion).

We can combine this model with the selection coefficient in Eq. 4 to quantify how much selection is amplified or diminished by correlated pleiotropy. That is, if a mutation changes growth rate by a small amount $\Delta g = g_2 - g_1$ from the wild-type, then according to Eq. 8 it will also change lag time by $\Delta\lambda \approx -a\Delta g/g^2$ and yield by $\Delta\nu = b\Delta g$, and hence the expected selection coefficient will be (using $\gamma = \Delta g/g$)

$$s \approx \gamma(\log\nu + a). \tag{9}$$

This shows that correlations between growth and yield have no effect on selection to leading order, since selection only depends logarithmically on yield. Correlations between growth and lag, however, can have a significant amplifying or diminishing effect. Since $\log\nu > 0$ always, synergistic pleiotropy ($a > 0$) will tend to increase the magnitude of selection, while antagonistic pleiotropy ($a < 0$) will tend to reduce it. The significance of this effect depends on the relative value of a compared to $\log\nu$; in general, the logarithm and the dimensionless nature of a suggest both should be order 1 and therefore comparable.

C. Selection is frequency-dependent

Equation 4 shows that the selection coefficient s depends on the initial frequency x of the mutant (Supplementary Methods, Fig. S2). This is fundamentally a consequence of having a finite resource: if resources were unlimited and selection were measured at some arbitrary time t instead of t_{sat} (which is intrinsically determined by the strains' growth traits), then the resulting selection coefficient would not depend on x.

This frequency-dependence means that some mutants are beneficial at certain initial frequencies and deleterious at others. The traits of these "conditionally-neutral" mutants must satisfy

$$\min(\nu_1, \nu_2) < e^{\omega(1+1/\gamma)} < \max(\nu_1, \nu_2), \tag{10}$$

which is obtained by determining which trait values allow $s(\tilde{x}) = 0$ for some frequency $0 < \tilde{x} < 1$. For mutants satisfying Eq. 10, the unique frequency at which the mutant is conditionally neutral is

$$\tilde{x} = \frac{\nu_1 e^{-\omega(1+1/\gamma)} - 1}{\nu_1/\nu_2 - 1}. \tag{11}$$

If the mutant and wild-type have equal yields ($\nu_1 = \nu_2 = \nu$), then the mutant is neutral at all frequencies if $e^{\omega(1+1/\gamma)} = \nu$. Mutants not satisfying these conditions are either beneficial at all frequencies ($s(x) > 0$) or deleterious at all frequencies ($s(x) < 0$).

D. Neutral, beneficial, and deleterious regions of mutant trait space

Figure 2A shows the regions of growth and lag trait space corresponding to conditionally-neutral (green), beneficial (blue), and deleterious (red) mutants. The steepness of the conditionally-neutral region is determined by the magnitudes of the yields: increasing both yields (e.g., by increasing the amount of resources R) makes the region more vertical, since that increases relative selection on growth (Eq. 6).

We can further understand the role of the yields by considering the trait space of growth rate and yield (Fig. 2B,C), as commonly considered in r/K selection studies. If the mutant has a longer lag time, then having a higher yield will be advantageous since the greater resource efficiency gives the mutant more time to grow exponentially to make up for its late start (Fig. 2B). On the other hand, if the the mutant has a shorter lag

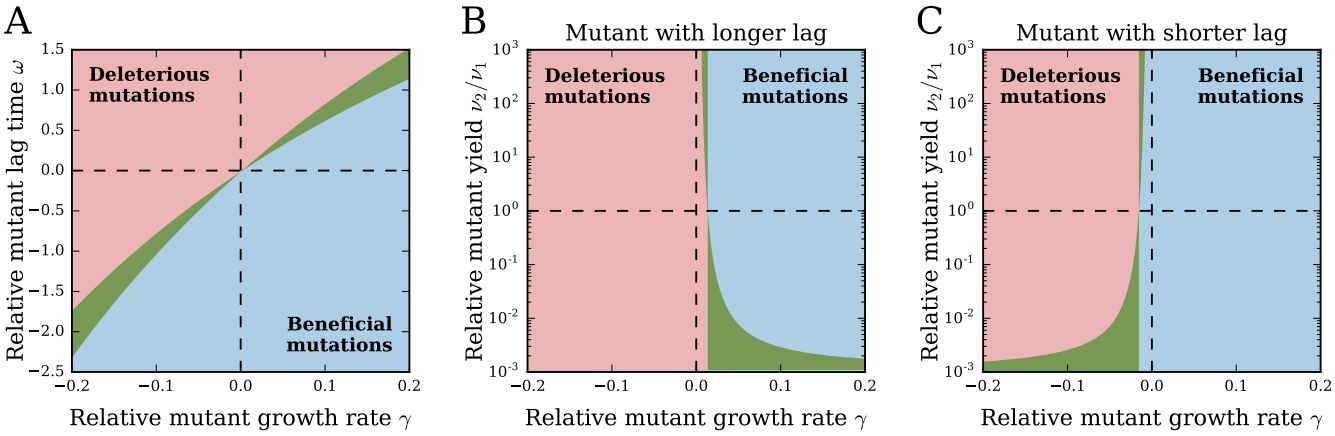

FIG. 2. Selection in mutant trait space. (A) Selection as a function of relative mutant growth rate $\gamma = (g_2 - g_1)/g_1$ and relative mutant lag time $\omega = (\lambda_2 - \lambda_1)g_1$. Mutants in the red region are deleterious ($s(x) < 0$) at all frequencies, while mutants in the blue region are beneficial ($s(x) > 0$) at all frequencies. Mutants in the green region are conditionally neutral, being beneficial at some frequencies and deleterious at others. Yield values are $\nu_1 = 10^3$ and $\nu_2 = 10^4$. (B) Same as (A) but in the trait space of relative mutant growth rate γ and relative mutant yield ν_2/ν_1, for a mutant with longer lag time ($\omega = 0.1$). (C) Same as (B) but for a mutant with shorter lag time ($\omega = -0.1$).

time, then having a lower yield is better since the mutant can hoard resources before the wild-type grows too much (Fig. 2C). These diagrams also show there are limits to how much changes in yield can affect selection: for example, if a deleterious mutant with slower growth ($\gamma < 0$) but shorter lag ($\omega < 0$) reduces its yield, the best it can do is become conditionally-neutral (move into the green region of Fig. 2C) — it can never become completely beneficial. Likewise, a beneficial mutant with faster growth but longer lag can never become completely deleterious by varying its yield (Fig. 2B). Furthermore, a mutant with worse growth *and* lag can never outcompete the wild-type, no matter how resource-efficient (high yield) it is. In this sense there are no pure "K-strategists" in the model [14]. Indeed, Eq. 4a indicates that there is no distinct selection pressure on yield, but rather it only modulates the relative selection pressures on growth versus lag. Note that increasing the mutant yield significantly above the wild-type value changes the selection coefficient very little, since the effective yield for the combined population (which determines the selection coefficient) is dominated by whichever strain is less-efficient through the harmonic mean in Eq. 4.

E. Frequency-dependent selection enables long-term coexistence of a mutant and wild-type

Mutants that are conditionally neutral (satisfying Eq. 10) will coexist with the wild-type at the frequency $\tilde{x}$ (Eq. 11). Figure 3A shows the conditionally-neutral region of trait space colored according to the coexistence frequency. The stability of coexistence depends on whether the selection coefficient increases or decreases as a function of frequency (Supplementary Methods). Stable coexistence requires a tradeoff between growth rate and yield — the mutant must have faster growth rate and lower yield, or slower growth rate and higher yield — in addition to the tradeoff between growth rate and lag time. Since Fig. 3A considers a mutant with yield higher than that of the wild-type, the lower branch of the coexistence region corresponds to mutants with stable coexistence, while mutants in the upper branch have unstable coexistence.

Given any two strains with different yields and a tradeoff between growth and lag, in principle it is always possible to construct competition conditions such that the two strains will coexist. That is, one may choose any coexistence frequency $\tilde{x}$ and use Eq. 7 to determine the critical value of the initial resources per cell R/N_0; with R/N_0 set to that value, the competition will have coexistence at precisely the desired frequency. Whether it is stable or unstable depends on whether there is a tradeoff between growth and yield.

Figure 3B shows the selection coefficients $s(x)$ as functions of frequency for two mutants with coexistence at $\tilde{x} = 1/2$, one that is stable (blue) and another that is unstable (red). The blue mutant has slower growth but shorter lag and higher yield compared to the wild-type. Therefore when the mutant is at low frequency (below the coexistence point), the overall yield of the combined population (harmonic mean in Eq. 4) is approximately equal to the wild-type's yield, and since the wild-type has lower yield, this results in stronger selection on lag versus growth. This means positive selection for the mutant, which has the shorter lag time. In contrast, when the mutant's frequency is high, the overall yield of the population is closer to the mutant's yield, and thus there is stronger selection on growth versus lag. This favors the wild-type strain, which has the faster growth rate,

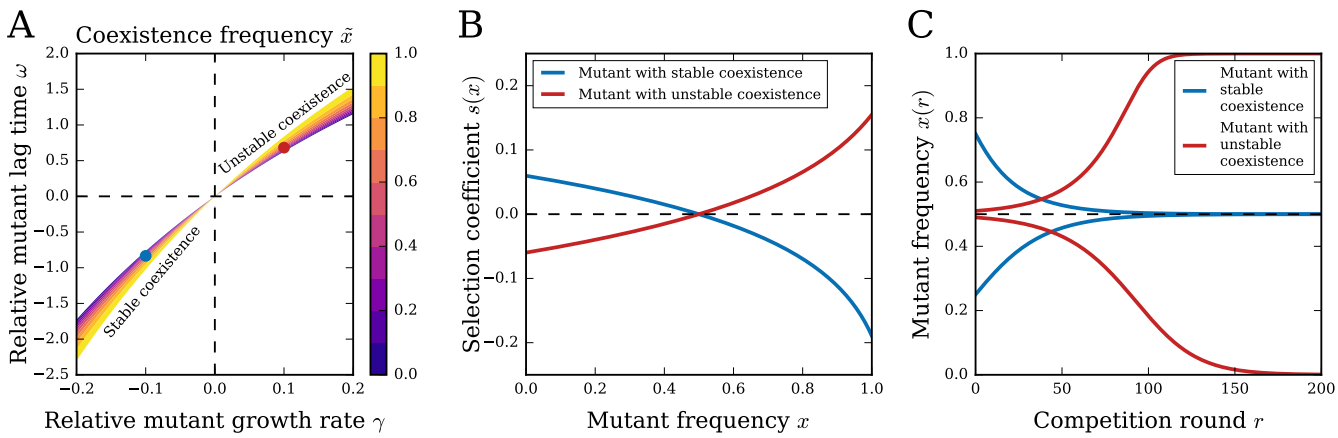

FIG. 3. Long-term coexistence of two strains. (A) Conditionally-neutral region of growth-lag trait space where coexistence occurs, colored by the coexistence frequency $\tilde{x}$ (Eq. 11). Since $\nu_2 > \nu_1$ in this example, mutants in the lower branch ($\gamma < 0$) of the conditionally-neutral region have stable coexistence, while mutants in the upper branch ($\gamma > 0$) have unstable coexistence. Blue and red points mark example mutants used in (B) and (C). (B) Selection coefficient $s(x)$ as a function of frequency x for mutants with coexistence at $\tilde{x} = 1/2$, where one mutant has stable coexistence (blue) and the other has unstable coexistence (red). (C) Mutant frequency $x(r)$ as a function of competition round r for two mutants with coexistence, each starting from two different initial conditions. The black dashed line marks the coexistence frequency $\tilde{x} = 1/2$. The yields are $\nu_1 = 10^3$ and $\nu_2 = 10^4$ in all panels.

and therefore produces negative selection on the mutant. These scenarios are reversed when the strain with faster growth (and longer lag) also has greater yield. In Fig. 3C we show example trajectories of the frequencies over rounds of competitions for these two mutants. Regardless of its initial frequency, the mutant with stable coexistence (blue) converges to coexistence with the wild-type, while the mutant with unstable coexistence (red) has opposite fates depending on whether its initial frequency starts above or below the coexistence frequency.

If the bottleneck population size N_0 at the beginning of each round is small, then stochastic effects of sampling from round to round (genetic drift) may be significant. We can gauge the robustness of stable coexistence to these fluctuations by comparing the magnitude of those fluctuations, which is of order $1/N_0$, with ds/dx measured at the coexistence frequency $\tilde{x}$ (Supplementary Methods), which estimates the strength of selection for a small change in frequency around coexistence. Coexistence will be robust against random fluctuations if

$$\left| \frac{\gamma(1-\nu_1/\nu_2)}{(1-\tilde{x}) + \tilde{x}(1+\gamma)\nu_1/\nu_2} \right| > \frac{1}{N_0}. \tag{12}$$

This tells us the critical value of the bottleneck size N_0, which we can control experimentally, needed to achieve robust coexistence. For example, if the mutant has 10% slower growth rate ($\gamma = -0.1$) but 10% higher yield ($\nu_2/\nu_1 = 1.1$), and coexistence occurs at $\tilde{x} = 1/2$, then N_0 must be greater than 100 for stabilizing selection at the coexistence frequency to be stronger than genetic drift.

Frequency-dependent selection may also significantly distort fixation of the mutant. In particular, it is common to measure selection on a mutant by competing the mutant against a wild-type starting from equal frequencies ($x = 1/2$) [27]. If selection is approximately constant across all frequencies, this single selection coefficient measurement $s(1/2)$ is sufficient to accurately estimate the fixation probability and time of the mutant (Supplementary Methods). However, mutants with coexistence may have fixation statistics that deviate significantly from this expectation due to frequency-dependent selection. For example, a mutant that coexists at $\tilde{x} = 1/2$ will have $s(1/2) = 0$ by definition, which would suggest the fixation probability of a single mutant should be the neutral value $\sim 1/N_0$. However, its fixation probability may actually be much lower than that when accounting for the full frequency-dependence of selection (Supplementary Methods, Fig. S3). Therefore accounting for the frequency-dependent nature of selection may be essential for predicting evolutionary fates of mutations with tradeoffs in growth traits.

F. Selection is non-additive and non-transitive

We now consider a collection of many strains with distinct growth traits. To determine all of their relative selection coefficients, in general we would need to perform binary competitions between all pairs. However, if selection obeys the additivity condition

$$s_{ij} + s_{jk} = s_{ik}, \tag{13}$$

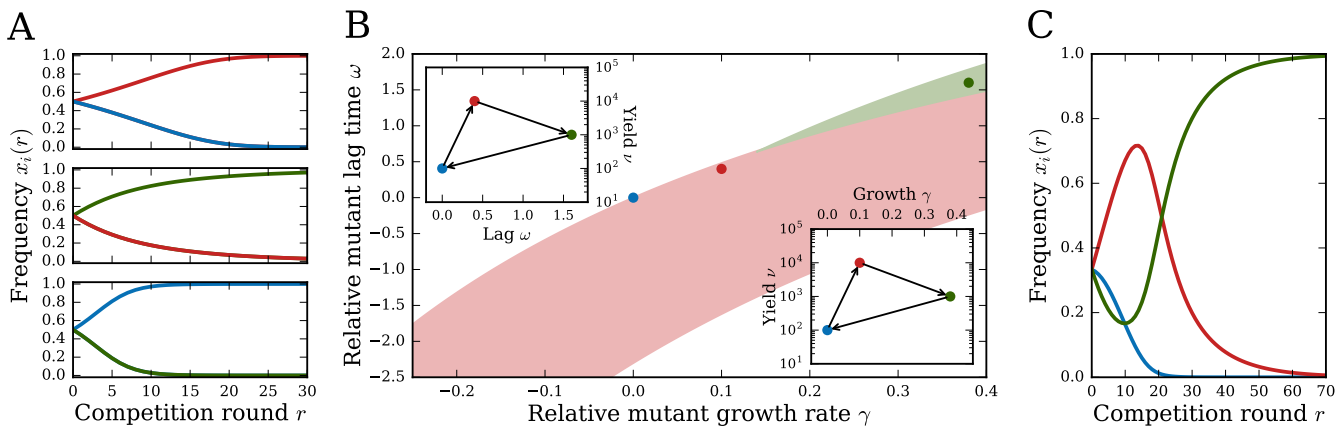

FIG. 4. Non-transitive selection over three strains. (A) An example of three strains (blue, red, green) forming a non-transitive set: in binary competitions starting from equal frequencies ($x = 1/2$), red beats blue, green beats red, and blue beats green. (B) The three strains from (A) in the trait space of relative growth rate γ and lag time ω (all relative to the blue strain); the red and green shaded regions indicate the available trait space for the red and green strains such that the three strains will form a non-transitive set. Insets: strains in the trait space of lag time and yield ν (upper left) and trait space of growth rate and yield (lower right). Arrows indicate which strain beats which in binary competitions. (C) Dynamics of each strain's frequency $x_i(r)$ over competition rounds r for all three strains in (A) simultaneously competing.

where s_{ij} is the selection coefficient of strain i over strain j in a binary competition, then we need only measure selection coefficients relative to a single reference strain, and from those we can predict selection for all other pairs. The additivity condition holds, for example, if selection coefficients are simply differences in scalar fitness values (Malthusian parameters) for each strain (i.e., $s_{ij} = f_i - f_j$). Therefore the extent to which Eq. 13 holds is indicative of the existence of such a fitness landscape.

Based on the selection coefficient definition (Eq. 2), the additivity condition would hold if the time t at which the selection coefficient is measured is a constant, independent of the two competing strains. In that case, there is a scalar fitness value $f_i = g_i(t - \lambda_i)$ for each strain, and the selection coefficients are just differences in these values (Supplementary Methods). However, if we only measure selection after the finite resources are exhausted, then the relevant time is the saturation time t_{sat}, which depends on the traits of the two competing strains and is therefore different for each binary competition. This means that the selection coefficient in this model does not obey additivity in general, although it will be approximately additive in the limit of small differences in growth traits between strains (Supplementary Methods).

A condition weaker than additivity is transitivity, which means that if strain 2 beats strain 1 and strain 3 beats strain 2 in binary competitions, then strain 3 must beat strain 1 in a binary competition as well [37]. This must also hold for neutrality, so if strains 1 and 2 are neutral, and strains 2 and 3 are neutral, then strains 1 and 3 must also be neutral. This essentially means that Eq. 13 at least predicts the correct sign for each binary selection coefficient.

If all three strains have equal yields, then selection in our model is always transitive for any initial frequencies (Supplementary Methods). If the yields are not all equal, then it is possible to find sets of three strains with non-transitive selection: each strain outcompetes one of the others in a binary competition (Supplementary Methods), forming a rock-paper-scissors game [38]. In Fig. 4A we show an example of three strains forming a non-transitive set. Figure 4B shows the distribution of these same three strains in trait space, where the shaded regions indicate constraints on the strains to exhibit non-transitivity. That is, given a choice of the blue strain's traits, the red strain's traits may lie anywhere in the red shaded region, which allows the red strain to beat the blue strain while still making it possible to choose the green strain and form a non-transitive set. Once we fix the red point, then the green strain's traits may lie anywhere in the green shaded regions.

This trait space diagram reveals what patterns of traits are conducive to generating non-transitive selection. The trait space constraints favor a positive correlation between growth rates and lag times across strains, indicating a growth-lag tradeoff. Indeed, these tradeoffs between growth strategies are the crucial mechanism underlying non-transitivity. For example, in Fig. 4A, red beats blue since red's faster growth rate and higher yield outweigh its longer lag time; green beats red due to its even faster growth rate, despite its longer lag and lower yield; and blue beats green with a shorter lag time and lower yield. Non-transitive strains will generally have no significant correlation between yield and growth rate or between yield and lag time (Fig. 4B, insets); furthermore, the cycle of selective advantage through the three strains generally goes clockwise in both the lag-yield and growth-yield planes.

Since each strain in a non-transitive set can beat one of the others in a binary competition, what will be the outcome in a competition with all three present? In Fig. 4C we show the ternary population dynamics for the non-transitive strains in Fig. 4A,B. Non-transitive and frequency-dependent selection creates complex population dynamics: the red strain rises at first, while the blue and green strains drop, but once blue is out of the way, that allows green to come back (since green loses to blue, but beats red) and eventually dominate over red. Note that we do not see oscillations or coexistence in these ternary competitions, as sometime occur with non-transitive interactions [37, 39].

IV. DISCUSSION

A. Selection on multiple growth phases produces complex population dynamics

Our model shows how basic properties of microbial growth cause the standard concept of a scalar fitness landscape to break down, revealing selection to depend fundamentally on the multidimensional nature of life history. This occurs even for the simple periodic environment (constant R and N_0) commonly used in laboratory evolution; fluctuating environments, as are expected in natural evolution, will likely exaggerate the importance of these effects. In contrast with previous theoretical work on tradeoffs between different phases of growth [19, 21], we have obtained simple mathematical results indicating the environmental conditions and patterns of traits necessary to produce complex population dynamics such as coexistence. In particular, we have shown how to tune the amount of resources R and bottleneck population size N_0 such that *any* pair of strains with a growth-lag tradeoff will coexist. We have also shown how frequency-dependent selection shapes mutant fixation, which was previously unexplored in this context [30]; indeed, the frequency dependence can skew the fixation probabilities and times by orders of magnitude compared to what would be expected from a measurement of selection at a single initial frequency (Fig. S3). Our model furthermore provides a simple mechanism for generating non-transitive interactions, in contrast to most known mechanisms that rely on particular patterns of allelopathy [38, 40], morphology [39], or spatial dynamics [41]. These results emphasize the need for more comprehensive measurements of selection beyond competition experiments against a reference strain at a single initial frequency [27]. As we have shown, these measurements may be insufficient to predict the long-term population dynamics at all frequencies (due to frequency-dependent selection), or the outcomes of all possible binary and higher-order competitions (due to non-transitive selection).

B. Pleiotropy and correlations between traits

Tradeoffs between growth and lag are necessary for coexistence and non-transitivity, while a tradeoff between growth and yield is necessary for coexistence to be stable. Whether these tradeoffs are commonly realized in an evolving microbial population largely depends on the pleiotropy of mutations. Two theoretical considerations suggest pleiotropy between growth and lag will be predominantly synergistic ($a > 0$ in Eq. 8). First, cell-to-cell variation in lag times [23, 24] means that the apparent population lag time is largely governed by the cells that happen to exit lag phase first and begin dividing, which causes the population lag time to be conflated with growth rate [32]. Second, mechanistic models that attempt to explain how growth rate and lag time depend on underlying cellular processes also predict synergistic pleiotropy [31, 34, 36]; conceptually, this is because the product of growth rate and lag time should be a positive constant corresponding to the amount of metabolic "work" (equal to a in Eq. 8) that the cell must perform to exit lag and begin to divide. Pleiotropy between growth rate and yield, on the other hand, is generally expected to be antagonistic ($b < 0$ in Eq. 8) due to thermodynamic constraints between the rate and yield of metabolic reactions [33, 35], although this constraint may not necessarily induce a correlation [42].

Distributions of these traits have been measured for both bacteria and fungi. Correlations between growth rate and yield have long been the focus of r/K selection studies; some of these experiments have indeed found tradeoffs between growth rate and yield [15–17, 35], but others have found no tradeoff, or even a positive correlation [5–7, 12, 13]. Measurements of lag times have also found mixed results [6, 11, 34, 36, 43]. However, the genetic versus environmental bases of these tradeoffs (or lack thereof) remain unclear [15], especially since these experiments are performed in different ways and make different types of comparisons (e.g., comparing multiple strains in the same environment, or comparing one strain across multiple environments). Furthermore, most of these data are for evolved populations, which may not reflect the true pleiotropy of mutations: distributions of fixed mutations may be correlated by selection even if the underlying distributions of mutations are uncorrelated. Our model shows that higher yield is only beneficial for faster growth rates, and so selection will tend to especially amplify mutations that increase both traits, which may explain some of the observed positive correlations between growth rate and yield. Indeed, data on the distributions of growth rates and yields from individual clones *within* a population shows a negative correlation [5]. The model developed here will be useful for further exploring the relationship between the underlying pleiotropy of mutations and the distribution of traits in evolved populations.

C. Analysis of experimental growth curves and competitions

Given a collection of microbial strains, we can measure their individual growth curves and determine growth rates, lag times, and yields. In principle, we can use the model (Eq. 4) to predict the outcome of any binary competition with these strains. In practice, however, there are several challenges in applying the model to this data. First, real growth dynamics are undoubtedly more complicated than the minimal model used here. There are additional time scales, such as the rate at which growth decelerates as resources are exhausted [19]; other frequency-dependent effects, such as a dependence of the lag time on the initial population size [44]; and more complex interactions between cells, such as cross-feeding [20]. In addition, the measured traits and competition parameters may be noisy, due to intrinsic noise within the cells as well as the extrinsic noise of the experiment.

Nevertheless, the simplicity of the model investigated here makes it a useful tool for identifying candidate strains from a collection of individual growth curves that may have interesting dynamics in pairs or in multi-strain competitions, which can then be subsequently tested by experiment. Existing technologies enable high-throughput measurement of individual growth curves for large numbers of strains [22–24], but systematic measurements of competitions are limited by the large number of possible strain combinations, as well as the need for sequencing or fluorescent markers to distinguish strains. The model can therefore help to target which competition experiments are likely to be most interesting by computationally scanning all combinations and setting bounds on various parameters to be compared with experimental uncertainties. For example, we can identify pairs of strains with growth-lag tradeoffs and predict a range of competition conditions R/N_0 that will lead to coexistence. We can also identify candidate sets of strains for demonstrating non-transitive selection. The model will be valuable for exploring these questions on large data sets of microbial growth traits.

ACKNOWLEDGMENTS

We thank Tommaso Biancalani, Parris Humphrey, and William Jacobs for valuable discussions, and Tal Einav for a critical reading of the manuscript. This work was supported by NIH awards F32 GM116217 to MM and R01 GM068670 to EIS.

AUTHOR CONTRIBUTIONS

MM, BVA, and EIS designed research; MM and BVA carried out calculations and analyzed data; MM wrote the manuscript. All authors edited and approved the final version.

[1] Orr HA. Fitness and its role in evolutionary genetics. Nat Rev Genet. 2009;10:531–539.
[2] McGill BJ, Enquist BJ, Weiher E, Westoby M. Rebuilding community ecology from functional traits. Trends Ecol Evol. 2006;21:178–185.
[3] Warmflash A, Francois P, Siggia ED. Pareto evolution of gene networks: an algorithm to optimize multiple fitness objectives. Phys Biol. 2012;9:56001.
[4] Vasi F, Travisano M, Lenski RE. Long-Term Experimental Evolution in Escherichia coli. II. Changes in Life-History Traits During Adaptation to a Seasonal Environment. Am Nat. 1994;144:432–456.
[5] Novak M, Pfeiffer T, Lenski RE, Sauer U, Bonhoeffer S. Experimental Tests for an Evolutionary Trade-Off between Growth Rate and Yield in E. coli. Am Nat. 2006;168:242–251.
[6] Warringer J, Zörgö E, Cubillos FA, Zia A, Gjuvsland A, Simpson JT, et al. Trait Variation in Yeast Is Defined by Population History. PLOS Genet. 2011;7:e1002111.
[7] Fitzsimmons JM, Schoustra SE, Kerr JT, Kassen R. Population consequences of mutational events: effects of antibiotic resistance on the r/K trade-off. Evol Ecol. 2010;24:227–236.
[8] Fridman O, Goldberg A, Ronin I, Shoresh N, Balaban NQ. Optimization of lag time underlies antibiotic tolerance in evolved bacterial populations. Nature. 2014;513:418–421.
[9] Reding-Roman C, Hewlett M, Duxbury S, Gori F, Gudelj I, Beardmore R. The unconstrained evolution of fast and efficient antibiotic-resistant bacterial genomes. Nat Ecol Evol. 2017;1:0050.
[10] Levin-Reisman I, Ronin I, Gefen O, Braniss I, Shoresh N, Balaban NQ. Antibiotic tolerance facilitates the evolution of resistance. Science. 2017;355:826–830.
[11] Adkar BV, Manhart M, Bhattacharyya S, Tian J, Musharbash M, Shakhnovich EI. Optimization of lag phase shapes the evolution of a bacterial enzyme. Nat Ecol Evol. 2017;1:0149.
[12] Luckinbill LS. r and K Selection in Experimental Populations of Escherichia coli. Science. 1978;202:1201–1203.
[13] Velicer GJ, Lenski RE. Evolutionary Trade-Offs Under Conditions of Resource Abundance and Scarcity: Experiments with Bacteria. Ecology. 1999;80:1168–1179.
[14] Reznick D, Bryant MJ, Bashey F. r- and K-selection revisited: The role of population regulation in life-history evolution. Ecology. 2002;83:1509–1520.
[15] Jasmin JN, Zeyl C. Life-History Evolution and Density-Dependent Growth in Experimental Populations of Yeast. Evolution. 2012;66:3789–3802.
[16] Jasmin JN, Dillon MM, Zeyl C. The yield of experimental yeast populations declines during selection. Proc R Soc B. 2012;279:4382–4388.
[17] Bachmann H, Fischlechner M, Rabbers I, Barfa N, dos Santos FB, Molenaar D, et al. Availability of public goods

shapes the evolution of competing metabolic strategies. Proc Natl Acad Sci USA. 2013;110:14302–14307.
[18] Levin BR. Coexistence of Two Asexual Strains on a Single Resource. Science. 1972;175:1272–1274.
[19] Stewart FM, Levin BR. Partitioning of Resources and the Outcome of Interspecific Competition: A Model and Some General Considerations. Am Nat. 1973;107:171–198.
[20] Turner PE, Souza V, Lenski RE. Tests of Ecological Mechanisms Promoting the Stable Coexistence of Two Bacterial Genotypes. Ecology. 1996;77:2119–2129.
[21] Smith HL. Bacterial competition in serial transfer culture. Math Biosci. 2011;229:149–159.
[22] Zackrisson M, Hallin J, Ottosson LG, Dahl P, Fernandez-Parada E, Ländström E, et al. Scan-o-matic: High-Resolution Microbial Phenomics at a Massive Scale. G3. 2016;6:3003–3014.
[23] Levin-Reisman I, Gefen O, Fridman O, Ronin I, Shwa D, Sheftel H, et al. Automated imaging with ScanLag reveals previously undetectable bacterial growth phenotypes. Nat Methods. 2010;7:737–739.
[24] Ziv N, Siegal ML, Gresham D. Genetic and Nongenetic Determinants of Cell Growth Variation Assessed by High-Throughput Microscopy. Mol Biol Evol. 2013;30:2568–2578.
[25] Zwietering MH, Jongenburger I, Rombouts FM, van 't Riet K. Modeling of the Bacterial Growth Curve. Appl Environ Microbiol. 1990;56:1875–1881.
[26] Buchanan RL, Whiting RC, Damert WC. When is simple good enough: a comparison of the Gompertz, Baranyi, and three-phase linear models for fitting bacterial growth curves. Food Microbiol. 1997;14:313–326.
[27] Elena SF, Lenski RE. Evolution experiments with microorganisms: the dynamics and genetic bases of adaptation. Nat Rev Genet. 2003;4:457–469.
[28] Crow JF, Kimura M. An Introduction to Population Genetics Theory. New York: Harper and Row; 1970.
[29] Chevin LM. On measuring selection in experimental evolution. Biol Lett. 2011;7:210–213.
[30] Wahl LM, Zhu AD. Survival Probability of Beneficial Mutations in Bacterial Batch Culture. Genetics. 2015;200:309–320.
[31] Baranyi J, Roberts TA. A dynamic approach to predicting bacterial growth in food. Int J Food Microbiol. 1994;23:277–294.
[32] Baranyi J. Comparison of Stochastic and Deterministic Concepts of Bacterial Lag. J Theor Biol. 1998;192:403–408.
[33] Pfeiffer T, Schuster S, Bonhoeffer S. Cooperation and Competition in the Evolution of ATP-Producing Pathways. Science. 2001;292:504–507.
[34] Swinnen IAM, Bernaerts K, Dens EJJ, Geeraerd AH, Impe JFV. Predictive modelling of the microbial lag phase: a review. Int J Food Microbiol. 2004;94:137–159.
[35] MacLean RC. The tragedy of the commons in microbial populations: insights from theoretical, comparative and experimental studies. Heredity. 2007;100:471–477.
[36] Himeoka Y, Kaneko K. Theory for Transitions Between Exponential and Stationary Phases: Universal Laws for Lag Time. Phys Rev X. 2017;7:021049.
[37] Verhoef HA, Morin PJ. Community Ecology: Processes, Models, and Applications. Oxford: Oxford University Press; 2010.
[38] Kerr B, Riley MA, Feldman MW, Bohannan BJM. Local dispersal promotes biodiversity in a real-life game of rock-paper-scissors. Nature. 2002;418:171–174.
[39] Sinervo B, Lively CM. The rock-paper-scissors game and the evolution of alternative male strategies. Nature. 1996;380:240–243.
[40] Jackson JBC, Buss L. Alleopathy and spatial competition among coral reef invertebrates. Proc Natl Acad Sci USA. 1975;72:5160–5163.
[41] Edwards KF, Schreiber SJ. Preemption of space can lead to intransitive coexistence of competitors. Oikos. 2010;119:1201–1209.
[42] Wong WW, Tran LM, Liao JC. A hidden square-root boundary between growth rate and biomass yield. Biotechnol Bioeng. 2009;102:73–80.
[43] Wang J, Atolia E, Hua B, Savir Y, Escalante-Chong R, Springer M. Natural Variation in Preparation for Nutrient Depletion Reveals a Cost-Benefit Tradeoff. PLOS Biol. 2015;13:e1002041.
[44] Kaprelyants AS, Kell DB. Do bacteria need to communicate with each other for growth? Trends Microbiol. 1996;4:237–242.

SUPPLEMENTARY METHODS

A. Minimal three-phase model of population growth

Let each strain i have lag time λ_i, growth rate g_i, and initial population size $N_i(0)$, so that its growth dynamics obey (Fig. 1A)

$$N_i(t) = \begin{cases} N_i(0) & 0 \le t < \lambda_i, \\ N_i(0)e^{g_i(t-\lambda_i)} & \lambda_i \le t < t_{\text{sat}}, \\ N_i(0)e^{g_i(t_{\text{sat}}-\lambda_i)} & t \ge t_{\text{sat}}. \end{cases} \tag{S1}$$

The time t_{sat} at which growth saturates is determined by a model of resource consumption. Let R be the total initial amount of resources. We assume that each strain consumes resources in proportion to its population size, for example, if the limiting resource is space. Let the yield Y_i be the number of cells of strain i per unit of the resource. Therefore the resources are exhausted at time $t = t_{\text{sat}}$ such that

$$\sum_i \frac{N_i(t_{\text{sat}})}{Y_i} = R. \tag{S2}$$

We can alternatively assume that each strain consumes resources in proportion to its total number of cell divisions, rather than its total number of cells. The number of cell divisions for strain i that have occurred by time t is $N_i(t) - N_i(0)$. Redefining the yield Y_i as the number of cell divisions per unit resource, saturation now occurs at the time $t = t_{\text{sat}}$ satisfying

$$\sum_i \frac{N_i(t_{\text{sat}}) - N_i(0)}{Y_i} = R. \tag{S3}$$

For simplicity we use the first model (Eq. S2) throughout this work, but it is straightforward to translate all results to the second model using the transformation $R \to R + \sum_i N_i(0)/Y_i$. This correction will generally be small, though, since $\sum_i N_i(0)/Y_i$ is the amount of resources that the initial population of cells consume for their first divisions, and this amount will usually be much less than the total resources R. It is also straightforward to further generalize this model to include other modes of resource consumption, such as consuming the resource per unit time during lag phase.

B. Instantaneous selection coefficient

The selection coefficient per unit time is

$$\sigma(t) = \frac{d}{dt} \log\left(\frac{N_2(t)}{N_1(t)}\right). \tag{S4}$$

In the minimal three-phase growth model (Eq. S1), we can write the growth curve as $N_i(t) = N_i(0)e^{g_i(t-\lambda_i)\Theta(t-\lambda_i)}$, where $\Theta(t)$ is the Heaviside step function. Then the instantaneous selection coefficient is:

$$\begin{aligned} \sigma(t) &= \frac{d}{dt}\Big[g_2(t-\lambda_2)\Theta(t-\lambda_2) - g_1(t-\lambda_1)\Theta(t-\lambda_1)\Big] \\ &= g_2\Theta(t-\lambda_2) - g_1\Theta(t-\lambda_1), \end{aligned} \tag{S5}$$

for $t < t_{\text{sat}}$, and $\sigma(t) = 0$ for $t > t_{\text{sat}}$.

Since we are mainly concerned with how the mutant frequency changes over whole cycles of growth, it is more convenient to integrate this instantaneous selection coefficient to obtain the total selection coefficient per cycle (Eq. 2):

$$\begin{aligned} s &= \int_0^{t_{\text{sat}}} dt\ \sigma(t) \\ &= \log\left(\frac{N_2(t_{\text{sat}})}{N_1(t_{\text{sat}})}\right) - \log\left(\frac{N_2(0)}{N_1(0)}\right). \end{aligned} \tag{S6}$$

C. Derivation of selection coefficient expression

In the minimal three-phase growth model (Eq. S1), the selection coefficient definition in Eq. 2 simplifies to

$$s = g_2(t_{\text{sat}} - \lambda_2) - g_1(t_{\text{sat}} - \lambda_1), \tag{S7}$$

excluding the trivial case where the time to saturation is less than one of the lag times (so that one strain does not grow at all). To determine how s explicitly depends on the underlying parameters, we must solve the saturation condition in Eq. S2 for t_{sat}:

$$R = \frac{N_0 x_1}{Y_1} e^{g_1(t_{\text{sat}}-\lambda_1)} + \frac{N_0 x_2}{Y_2} e^{g_2(t_{\text{sat}}-\lambda_2)}, \tag{S8}$$

where N_0 is the total initial population size and x_1, x_2 are the initial frequencies of the wild-type and mutant. While we cannot analytically solve this equation in general, we can obtain a good approximation in the limit of weak selection ($|s| \ll 1$). First we rewrite the equation in terms of the selection coefficient using Eq. S7:

$$R = N_0 e^{g_1(t_{\text{sat}}-\lambda_1)} \left(\frac{x_1}{Y_1} + \frac{x_2}{Y_2} e^{s}\right). \tag{S9}$$

We then solve for t_{sat} and expand to first order in s:

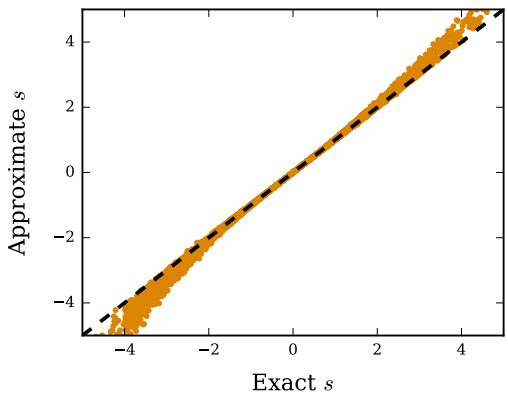

FIG. S1. Comparison of the approximate selection coefficient formula (Eq. 4) with the exact result obtained using the definition in Eq. 2 and a numerical solution to the saturation equation (Eq. S8). Each orange point corresponds to a different set of randomly-generated growth traits (γ, ω, ν_1, ν_2; see Eq. 1) and initial mutant frequencies x. The black dashed line is the line of identity.

$$t_{\text{sat}} \approx \lambda_1 - \frac{1}{g_1}\log\left[\frac{N_0}{R}\left(\frac{x_1}{Y_1}+\frac{x_2}{Y_2}\right)\right] - \frac{x_2/Y_2}{g_1(x_1/Y_1+x_2/Y_2)}s. \quad \text{(S10)}$$

For self-consistency this expression for t_{sat} should be invariant under exchange of the mutant and wild-type indices and switching the sign of s; equating these two equivalent expressions for t_{sat} allows us to solve for s, which gives the main result in Eq. 4.

In Fig. S1 we compare the selection coefficient calculated from this approximate expression with the exact result obtained by numerically solving Eq. S8 for t_{sat} and then directly calculating s using the definition of Eq. 2. This empirically shows that although the derivation relies on the approximation of weak selection ($|s| \ll 1$), Eq. 4 is extremely accurate over a wide range of parameter values, even up to rather strong selection strengths $|s| \sim 1$. Furthermore, the expression is exact in two special cases: when the mutant and the wild-type are selectively neutral ($s = 0$), and when the mutant and wild-type have equal growth rates ($g_1 = g_2 = g$), since $s = -(\lambda_2 - \lambda_1)g = -\omega$ according to Eq. S7.

D. Saturation time and total population size

Here we derive expressions for the saturation time t_{sat} and the total population size at saturation

$$\begin{aligned} N_{\text{sat}} &= N_1(t_{\text{sat}}) + N_2(t_{\text{sat}}) \\ &= N_0 x_1 e^{g_1(t_{\text{sat}}-\lambda_1)} + N_0 x_2 e^{g_2(t_{\text{sat}}-\lambda_2)}. \end{aligned} \quad \text{(S11)}$$

We assume the nontrivial case of $t_{\text{sat}} > \lambda_1, \lambda_2$. First, if the growth rates are equal ($g_1 = g_2 = g$), we can obtain exact solutions since the two-strain saturation condition (Eq. S8) is analytically solvable for t_{sat}:

$$\begin{aligned} t_{\text{sat}} &= \frac{1}{g}\log\left[\frac{R}{2N_0}H\left(\frac{Y_1 e^{g\lambda_1}}{x_1}, \frac{Y_2 e^{g\lambda_2}}{x_2}\right)\right], \\ N_{\text{sat}} &= \frac{1}{2}(x_1 e^{-g\lambda_1} + x_2 e^{-g\lambda_2}) H\left(\frac{RY_1 e^{g\lambda_1}}{x_1}, \frac{RY_2 e^{g\lambda_2}}{x_2}\right). \end{aligned} \quad \text{(S12)}$$

If the growth rates are unequal ($g_1 \neq g_2$), then we must rely on the small s approximation. We can rearrange Eq. S7 to obtain t_{sat} as a function of s:

$$t_{\text{sat}} = \frac{s + g_2\lambda_2 - g_1\lambda_1}{g_2 - g_1}. \quad \text{(S13)}$$

We can then substitute the approximate expression for s (Eq. 4) into Eq. S13:

$$t_{\text{sat}} \approx \left(\frac{x_1/Y_1 + x_2/Y_2}{g_1 x_1/Y_1 + g_2 x_2/Y_2}\right)\left(\log\left[\frac{R}{2N_0}H\left(\frac{Y_1}{x_1}, \frac{Y_2}{x_2}\right)\right] - \frac{g_1 g_2(\lambda_2 - \lambda_1)}{g_2 - g_1}\right) + \frac{g_2\lambda_2 - g_1\lambda_1}{g_2 - g_1}. \quad \text{(S14)}$$

To obtain an expression for N_{sat} in this approximation, we rewrite its definition (Eq. S11) in terms of s using Eq. S13:

$$N_{\text{sat}} = N_0 e^{g_1 g_2(\lambda_2-\lambda_1)/(g_2-g_1)} \times \left(x_1 e^{g_1 s/(g_2-g_1)} + x_2 e^{g_2 s/(g_2-g_1)}\right). \quad \text{(S15)}$$

For small s, we can show from Eq. 4 that

$$\begin{aligned} e^{g_1 g_2(\lambda_2-\lambda_1)/(g_2-g_1)} &\approx \frac{1}{2N_0}H\left(\frac{RY_1}{x_1}, \frac{RY_2}{x_2}\right)\exp\left[-\left(\frac{s}{g_2-g_1}\right)\left(\frac{g_1 x_1/Y_1 + g_2 x_2/Y_2}{x_1/Y_1 + x_2/Y_2}\right)\right] \\ &\approx \frac{1}{2N_0}H\left(\frac{RY_1}{x_1}, \frac{RY_2}{x_2}\right)\left[1 - \left(\frac{s}{g_2-g_1}\right)\left(\frac{g_1 x_1/Y_1 + g_2 x_2/Y_2}{x_1/Y_1 + x_2/Y_2}\right)\right] \end{aligned} \quad \text{(S16)}$$

Substituting this into Eq. S15 and expanding to first order in s shows that the saturation population size is ap-

proximately

$$N_{\text{sat}} \approx \frac{1}{2} H\left(\frac{RY_1}{x_1}, \frac{RY_2}{x_2}\right) \times \left[1 - \frac{x_1 x_2 (Y_2^{-1} - Y_1^{-1})}{x_1/Y_1 + x_2/Y_2} s\right]. \quad \text{(S17)}$$

Therefore the saturation size in the neutral case ($s = 0$) is

$$\begin{aligned} N_{\text{sat}} &= \frac{1}{2} H\left(\frac{RY_1}{x_1}, \frac{RY_2}{x_2}\right) \\ &= H\left(\frac{N_{\text{sat},1}}{2x_1}, \frac{N_{\text{sat},2}}{2x_2}\right), \end{aligned} \quad \text{(S18)}$$

since $RY_i = N_{\text{sat},i}$, where $N_{\text{sat},i}$ is the saturation population size of strain i if no other strains are present. So for a neutral pair of strains, the total population grows to the harmonic mean of the saturation population sizes of the individual strains; this shows that we can interpret the harmonic mean of both strains' yields as the effective yield for the combined population. When selection is nonzero, the effective yield is perturbed above this value if the strain with higher yield is also positively selected (e.g., $Y_2 > Y_1$ and $s > 0$), while otherwise it is perturbed below the neutral value.

E. Frequency-dependence of selection

The selection coefficient in Eq. 4 depends on the initial mutant frequency x. Here we show that $s(x)$ is a monotonic function of the frequency x; this is important because it means that coexistence ($s(x) = 0$) occurs at a unique frequency $\tilde{x}$ (Eq. 11). We use an exact argument starting from the original model because the approximate $s(x)$ function in Eq. 4 has spurious non-monotonic behavior in some regimes. For simplicity we again use the dimensionless growth parameters defined in Eq. 1.

If the mutant and wild-type have equal growth rates ($\gamma = 0$), then we have previously showed that $s(x) = -\omega$, so it is constant (and hence monotonic) in x. Now we consider $\gamma \neq 0$. In this case we can write the saturation condition in terms of $s(x)$ by substituting Eq. S13 for t_{sat} in Eq. S8:

$$e^{\omega(1+\gamma)/\gamma}\left[\frac{(1-x)}{\nu_1} e^{s(x)/\gamma} + \frac{x}{\nu_2} e^{(1+1/\gamma)s(x)}\right] = 1. \quad \text{(S19)}$$

We can differentiate with respect to x and solve for ds/dx to obtain the differential equation

$$\frac{ds}{dx} = \frac{\gamma\left(1 - \frac{\nu_1}{\nu_2} e^{s(x)}\right)}{(1-x) + x(1+\gamma)\frac{\nu_1}{\nu_2} e^{s(x)}}. \quad \text{(S20)}$$

The only way $s(x)$ can be non-monotonic is if $ds/dx = 0$ for some x without $s(x)$ being constant. Since the denominator of Eq. S20 is always positive, $ds/dx = 0$ only if $s(x) = \log(\nu_2/\nu_1)$ for some x. However, if $s(x) = \log(\nu_2/\nu_1)$ for any x, then it must be constant at $\log(\nu_2/\nu_1)$ for all x. We show this by substituting $s(x) = \log(\nu_2/\nu_1)$ into the saturation equation (Eq. S19). The x-dependence drops out and we are left with

$$\frac{\nu_2^{1/\gamma}}{\nu_1^{1+1/\gamma}} e^{\omega(1+1/\gamma)} = 1. \quad \text{(S21)}$$

Therefore if the parameters satisfy this condition, then $s(x) = \log(\nu_2/\nu_1)$ for all x. Therefore ds/dx only equals zero when $s(x)$ is constant, and so $s(x)$ can never be a non-monotonic function of x.

Figure S2A shows the sign of ds/dx over growth-lag trait space for strains with equal yields ($\nu_1 = \nu_2$); Fig. S2B shows the case of unequal yields ($\nu_1 \neq \nu_2$). The boundaries between signs of ds/dx are where $s(x)$ is a constant, and thus they are given by $\gamma = 0$ and Eq. S21. Note that for equal yields, $s(x)$ is constant at zero along the neutral boundary (Fig. S2A), whereas for unequal yields there is a separate boundary, away from the conditionally-neutral region, where $s(x)$ has a constant but nonzero value (Fig. S2B).

Another way to measure the frequency-dependence of selection is to consider its total variation across the whole range of frequencies. We define the relative variation of selection as $|(s_{\max} - s_{\min})/s(1/2)|$, where $s_{\max}$ and $s_{\min}$ are the maximum and minimum values of $s(x)$ across all frequencies, and $s(1/2)$ is selection at the intermediate frequency $x = 1/2$. Since $s(x)$ is always a monotonic function of x, the maximum and minimum values are attained at the endpoints $x = 0$ and $x = 1$. The selection coefficient is not technically defined for these values (since either the mutant or the wild-type is extinct), but we can determine its value in the limits $x \to 0$ and $x \to 1$. In the limit of $x \to 0$, the saturation time must be the time for the wild-type alone to consume all the resources, and vice-versa for $x \to 1$:

$$\begin{aligned} \lim_{x\to 0} t_{\text{sat}}(x) &= \lambda_1 + \frac{1}{g_1}\log\left(\frac{RY_1}{N_0}\right), \\ \lim_{x\to 1} t_{\text{sat}}(x) &= \lambda_2 + \frac{1}{g_2}\log\left(\frac{RY_2}{N_0}\right). \end{aligned} \quad \text{(S22)}$$

Using the relationship between s and t_{sat} in Eq. S7 and converting to dimensionless parameters (Eq. 1), we have

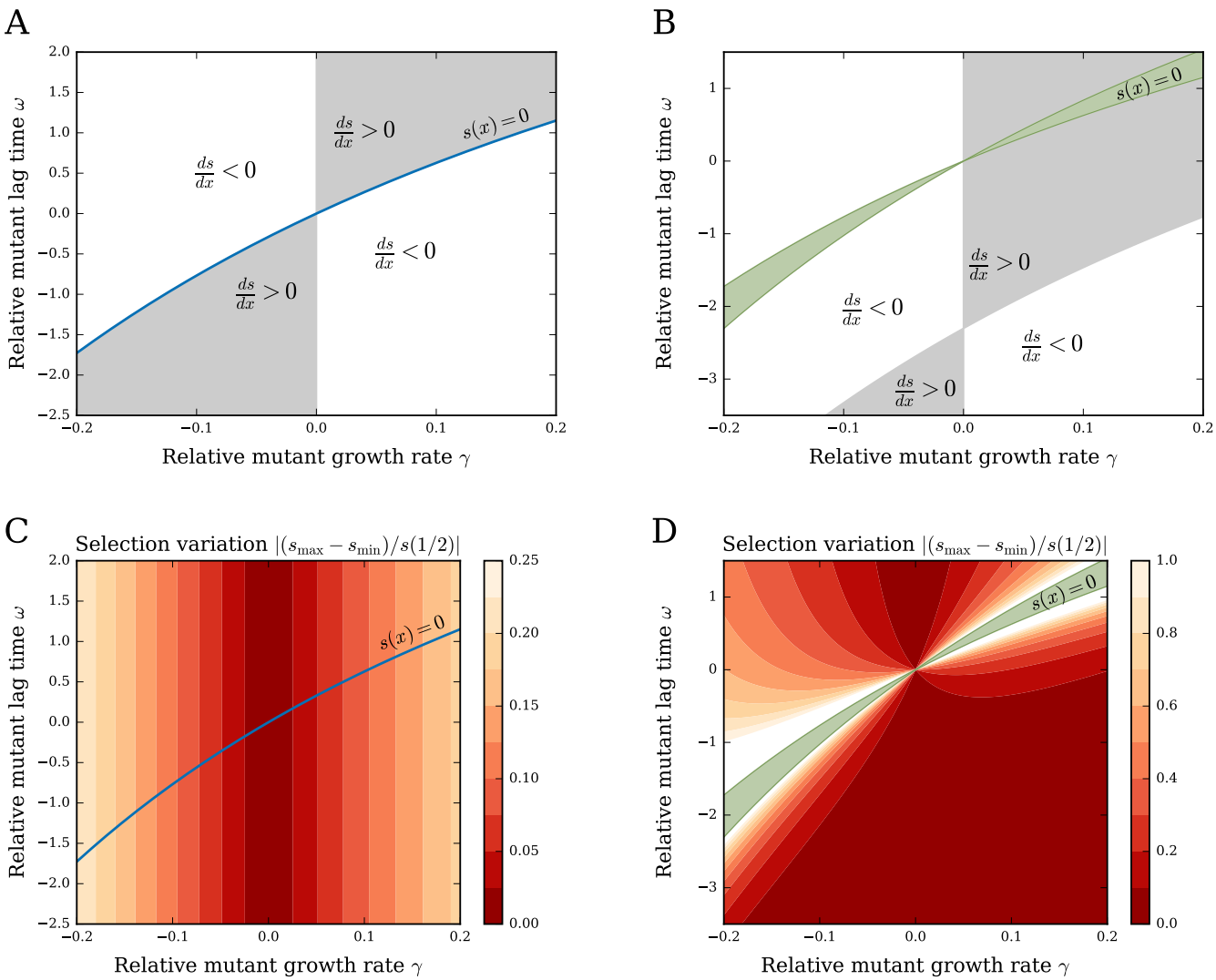

FIG. S2. Frequency-dependence of the selection coefficient over growth-lag trait space. (A) For a mutant and wild-type with equal yields ($\nu_1 = \nu_2 = 10^3$), the gray and white regions indicate where the selection coefficient $s(x)$ increases as a function of mutant frequency ($ds/dx > 0$) or decreases ($ds/dx < 0$). The neutral boundary is in blue. (B) Same as (A) but for a mutant and wild-type with unequal yields ($\nu_1 = 10^3$, $\nu_2 = 10^4$). The conditionally-neutral region is shown in green. (C) Relative variation of the selection coefficient over mutant frequencies when the mutant and wild-type have equal yields. Yield values and the neutral boundary are the same as (A). (D) Same as (C) but for a mutant and wild-type with unequal yields; yield values and the conditionally-neutral region are the same as (B). The relative variation diverges in the conditionally-neutral region since $s(1/2) = 0$ for some points.

$$\lim_{x\to 0} s(x) = \gamma \log \nu_1 - \omega(1+\gamma),$$
$$\lim_{x\to 1} s(x) = \left(\frac{\gamma}{1+\gamma}\right) \log \nu_2 - \omega. \tag{S23}$$

Hence the total variation of selection coefficients is

$$|s_{\max} - s_{\min}| = \left|\lim_{x\to 1} s(x) - \lim_{x\to 0} s(x)\right| = \left|\gamma\left(\frac{\log \nu_2}{1+\gamma} - \log \nu_1 + \omega\right)\right|. \tag{S24}$$

This result is exact (no weak selection approximation), but the approximate $s(x)$ expression in Eq. 4 gives an identical result.

Normalizing this total range of selection by its magnitude at some intermediate frequency, such as $x = 1/2$,

measures the relative variation in $s(x)$ over frequencies. For equal yields ($\nu_1 = \nu_2$), the relative variation simplifies to

$$\left|\frac{s_{\max} - s_{\min}}{s(1/2)}\right| = \left|\frac{\gamma(2+\gamma)}{2(1+\gamma)}\right|. \tag{S25}$$

It is small over a large range of the trait space (Fig. S2C), indicating that the frequency-dependence of selection is relatively weak for equal yields. In contrast, when the yields are unequal ($\nu_1 \neq \nu_2$), the variation becomes very large near the conditionally-neutral region (Fig. S2D). This is because $s(1/2)$ goes to zero for some points in the conditionally-neutral region, while the total range $|s_{\max} - s_{\min}|$ remains finite. Thus, the frequency-dependence of selection is most significant for mutants in the conditionally-neutral region; this is expected since these are the mutants that can coexist with the wild-type.

F. Fixation under frequency-dependent selection

If the population at the end of a competition round is randomly sampled to populate the next round, this is equivalent to a Wright-Fisher process with frequency-dependent selection coefficient $s(x)$ and effective population size N_0 [28]. In the limit of a large population ($N_0 \gg 1$) and weak selection ($|s(x)| \ll 1$), the fixation probability of a mutant starting from frequency x is

$$\phi(x) = \frac{\int_0^x dx'\ e^{2N_0 V(x')}}{\int_0^1 dx'\ e^{2N_0 V(x')}}, \tag{S26}$$

where $V(x)$ is the effective selection "potential":

$$V(x) = -\int_0^x dx'\ s(x'). \tag{S27}$$

This is defined in analogy with physical systems, where selection plays the role of a force and $V(x)$ is the corresponding potential energy function. The mean time (number of competition rounds) to fixation, given that fixation eventually occurs, is

$$\theta(x) = \int_x^1 dx'\ \psi(x')\phi(x')(1-\phi(x')) + \left(\frac{1-\phi(x)}{\phi(x)}\right)\int_0^x dx'\ \psi(x')\left(\phi(x')\right)^2, \tag{S28}$$

where

$$\psi(x) = \frac{2N_0 e^{-2N_0 V(x)}}{x(1-x)}\int_0^1 dx'\ e^{2N_0 V(x')}. \tag{S29}$$

These results assume that mutations are rare enough to neglect interference from multiple *de novo* mutations.

For simplicity we focus on the case of a single mutant cell (frequency $1/N_0$) at the beginning of a competition round. To test the effect of frequency-dependence on fixation, we compare the true fixation probabilities and times, calculated from Eqs. S26 and S28 using $s(x)$ (Eq. 4), with the fixation probabilities and times predicted if selection has a constant value at $s(1/2)$, as is often measured in competition experiments [27]. When selection is a constant across frequencies, Eq. S26 simplifies to Kimura's formula [28]:

$$\phi(1/N_0) = \frac{1-e^{-2s}}{1-e^{-2N_0 s}}. \tag{S30}$$

Deviations from this relationship between ϕ and $s(1/2)$ are therefore indicative of significant frequency-dependence.

For several sets of mutants, Fig. S3A shows their measured selection coefficients $s(1/2)$ versus their fixation probabilities $\phi(1/N_0)$. In orange are mutants obtained by uniformly scanning a rectangular region of growth-lag trait space (e.g., the trait space shown in Fig. 2A). The black line shows the prediction from Kimura's formula (Eq. S30) assuming $s = s(1/2)$ is a constant selection coefficient for all frequencies; this frequency-independent approximation appears to describe these mutants well. The mean fixation times $\theta(1/N_0)$ (Fig. S3B) for these mutants are also well-described by assuming constant selection coefficient $s(1/2)$. This is because the frequency-dependence for these mutants is weak, as shown in Fig. S2C,D. Therefore a single measurement of the selection coefficient for these mutants at any initial frequency provides an accurate prediction of the long-term population dynamics.

The plots of selection variation in Fig. S2C,D indicate that the most significant frequency-dependence occurs for mutants in the conditionally-neutral region with unequal yields, i.e., mutants with coexistence. We thus calculate the fixation probabilities and times for mutants with coexistence at particular frequencies, and compare these statistics to their selection coefficients at $x = 1/2$ as would be measured experimentally. As expected, the fixation statistics show significant deviations from the predictions for constant selection. In particular, mutants with coexistence at $\tilde{x} = 1/2$ (Eq. 11) have $s(1/2) = 0$ by definition, but they nevertheless show a wide range of fixation probabilities and times, some above the neutral values ($\phi = 1/N_0$, $\theta = 2N_0$) and some below.

Figure S3C,D shows the fixation probabilities and times of mutants with coexistence as functions of their relative growth rates γ, which separates mutants with stable coexistence from those with unstable coexistence: the mutant has higher yield than that of the wild-type in this example ($\nu_2 > \nu_1$), so the mutants with worse growth rate ($\gamma < 0$) have stable coexistence while the mutants with better growth rate ($\gamma > 0$) are unstable. Mutants

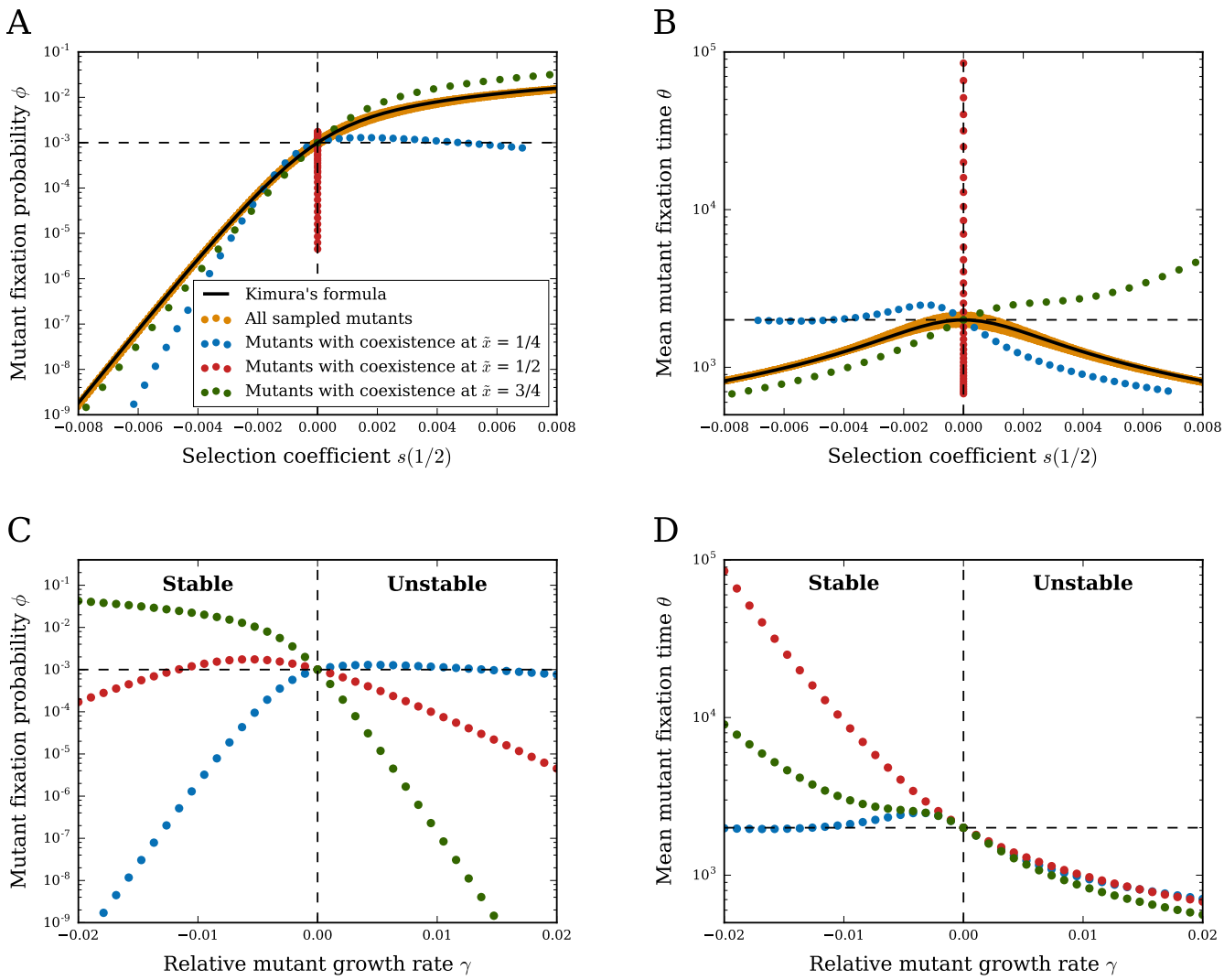

FIG. S3. Mutant fixation probabilities and times. (A) Fixation probability $\phi(1/N_0)$ as a function of the selection coefficient at frequency $x = 1/2$. Orange points correspond to mutants uniformly sampled across a rectangular region of growth-lag trait space: $(\gamma, \omega) \in [-10^{-3}, 10^{-3}] \times [-5 \times 10^{-3}, 5 \times 10^{-3}]$. Other points correspond to mutants with coexistence at specific frequencies (blue for $\tilde{x} = 1/4$, red for $\tilde{x} = 1/2$, green for $\tilde{x} = 3/4$). We calculate fixation probabilities using the frequency-dependent selection coefficient $s(x)$ (Eq. 4) and Eq. S26; for comparison, the solid black line indicates the prediction from Kimura's formula (Eq. S30), assuming a frequency-independent selection coefficient. The horizontal dashed line marks the neutral fixation probability $\phi = 1/N_0$. (B) Same as (A), but with the mean fixation time $\theta(1/N_0)$ (conditioned on eventual fixation) on the vertical axis. The solid black line marks the prediction for a frequency-independent selection coefficient (Eq. S28), and the horizontal dashed line marks the neutral fixation time $\theta = 2N_0$. (C) Fixation probability $\phi(1/N_0)$ as a function of the relative growth rate γ for mutants with coexistence. Colors indicate the same coexistence frequencies as in (A) and (B). Mutants with $\gamma < 0$ have stable coexistence, while mutants with $\gamma > 0$ have unstable coexistence (since $\nu_2 > \nu_1$). Dashed lines are the same as in (A). (D) Same as (C), but with the mean fixation time $\theta(1/N_0)$ on the vertical axis. Dashed lines are the same as (B). In all panels, the relative yields are $\nu_1 = 10^3$ and $\nu_2 = 10^4$, and the initial population size is $N_0 = 10^3$.

with unstable coexistence at $\tilde{x} = 1/2$ fix with lower probability than would a purely neutral mutant (Fig. S3C), but if they do fix, they do so in less time (Fig. S3D). We can understand this in analogy with diffusion across an energy barrier, using the effective selection potential defined in Eq. S27. The mutant starts at frequency $1/N_0$, and to reach fixation it must not only survive fluctuations from genetic drift while at low frequency, but it also must cross the effective selection potential barrier at the coexistence frequency. Indeed, the mutant is actually deleterious at low frequencies (below the coexistence frequency), and thus we expect the fixation probability to be lower than that of a purely neutral mutant. If such a mutant does fix, though, it will do so rapidly, since it requires rapid fluctuations from genetic drift to cross the selection barrier. This effect is most pronounced for coex-

istence at relatively high frequencies; for low coexistence frequencies, such as $\tilde{x} = 1/4$, the barrier is sufficiently close to the initial frequency $1/N_0$ that it is easier to cross, and thus the fixation probability is closer to the neutral value (Fig. S3C).

Mutants with stable coexistence, on the other hand, are described by a potential well at the coexistence frequency. The fixation of these mutants is determined by a tradeoff between the initial boost of positive selection toward the coexistence frequency, which helps to avoid immediate extinction, and the stabilizing selection they experience once at coexistence. In particular, once at the coexistence frequency, the mutant must eventually cross a selection barrier to reach either extinction or fixation. However, the barrier to fixation is always higher, and thus the mutant has a greater chance of going extinct rather than fixing. As we see for mutants with stable coexistence at $\tilde{x} = 1/2$, decreasing γ from zero initially improves the probability of fixation over neutrality, but eventually it begins to decrease. Thus, the frequency-dependence of mutants with coexistence plays a crucial role in shaping their fixation statistics, and their ultimate fates depend crucially on their individual trait values (i.e., γ).

G. Additivity of the selection coefficient

The additivity condition (Eq. 13) is approximately satisfied if strains i, j, and k have only small differences in growth rates, lag times, and yields. Conceptually, this is because the saturation times t_{sat} for each binary competition between pairs of strains are all approximately equal, but we can also show this directly using the selection coefficient formula. Let $\gamma_{ij} = (g_i - g_j)/g_j$, $\omega_{ij} = (\lambda_i - \lambda_j)g_j$, and $\mu_{ij} = (\nu_i - \nu_j)/\nu_j$ be the relative differences in growth rate, lag time, and yield for strains i and j. If these relative differences are all small, then they each approximately obey the additivity condition across strains:

$$\begin{aligned} \gamma_{ik} &= (1+\gamma_{ij})(1+\gamma_{jk}) - 1 && \approx \gamma_{ij} + \gamma_{jk}, \\ \omega_{ik} &= \frac{\omega_{ij}}{1+\gamma_{jk}} + \omega_{jk} && \approx \omega_{ij} + \omega_{jk}, \\ \mu_{ik} &= (1+\mu_{ij})(1+\mu_{jk}) - 1 && \approx \mu_{ij} + \mu_{jk}. \end{aligned} \tag{S31}$$

In this same limit, the total selection coefficient for strains i and j is approximately

$$s_{ij} \approx \gamma_{ij} \log \nu_j - \omega_{ij}. \tag{S32}$$

Note that, to leading order, the change in yield μ_{ij} does not appear. Using Eq. S31 and $\nu_j = (1+\mu_{jk})\nu_k$, we have

$$\begin{aligned} s_{ij} + s_{jk} &\approx \gamma_{ij} \log \nu_j - \omega_{ij} + \gamma_{jk} \log \nu_k - \omega_{jk} \\ &\approx \gamma_{ik} \log \nu_k - \omega_{ik} \\ &\approx s_{ik}. \end{aligned} \tag{S33}$$

Therefore the selection coefficient is approximately additive when differences between traits are small.

H. Transitivity of the selection coefficient

Since we are only concerned with the sign of selection in determining transitivity, we focus on the signed component of the selection coefficient in Eq. 4. It is also more convenient to use growth times $\tau_i = 1/g_i$ rather than growth rates, and the quantity $h_{ij} = \log \frac{1}{2} H(\frac{\nu_j}{1-x}, \frac{\nu_i}{x})$ for the logarithm of the harmonic mean yield. We define the signed component of the selection coefficient for strain i over strain j to be

$$(\tau_j - \tau_i)h_{ij} + \lambda_j - \lambda_i. \tag{S34}$$

That is, s_{ij} is proportional to this quantity up to an overall factor that is always nonnegative.

We first consider whether neutrality is a transitive property of strains. Three strains are all pairwise neutral if their traits satisfy

$$\begin{aligned} (\tau_1 - \tau_2)h_{12} + \lambda_1 - \lambda_2 &= 0, \\ (\tau_2 - \tau_3)h_{23} + \lambda_2 - \lambda_3 &= 0, \\ (\tau_3 - \tau_1)h_{13} + \lambda_3 - \lambda_1 &= 0. \end{aligned} \tag{S35}$$

If all three strains have equal yields $\nu_1 = \nu_2 = \nu_3$ ($h_{12} = h_{23} = h_{13}$ for all frequencies), then any two of these equations imply the third (e.g., by adding them together), which means that neutrality is transitive when all strains have equal yields. If two of the yields are equal while the third is distinct, then transitivity only holds if two of the strains are identical (equal growth and lag times). For example, if $\nu_1 = \nu_2 \neq \nu_3$, then we can add together the last two equations in Eq. S35 to obtain

$$(\tau_2 - \tau_1)h_{13} + \lambda_2 - \lambda_1 = 0, \tag{S36}$$

(using $h_{23} = h_{13}$), but this is only consistent with the first equation in Eq. S35 if $\tau_1 = \tau_2$ and $\lambda_1 = \lambda_2$, i.e., strains 1 and 2 are identical in all traits.

If all the yields have distinct values, then transitivity will generally not hold for arbitrary values of the growth traits. However, it is still *possible* for three strains with distinct yields to all be pairwise neutral, but only with very specific values of the traits. Note that with unequal yields, neutrality at all frequencies is not possible, so pairs of strains are only conditionally-neutral, with

coexistence (stable or unstable) at some particular frequency. These frequencies are encoded in the quantities h_{ij}. We thus fix the yields and the desired coexistence frequencies to arbitrary values, and without loss of generality, we can assume $h_{12} < h_{13} < h_{23}$ (e.g., by putting the strains in order of increasing yields). We can also choose any values of τ_1 and λ_1 since this amounts to a rescaling and shift of time units. Therefore we are left with three linear equations (Eq. S35) for four unknowns: $\tau_2, \tau_3, \lambda_2, \lambda_3$. If we choose any value of the strain 2 growth time that obeys

$$\tau_2 > \left(\frac{h_{13} - h_{12}}{h_{23} - h_{12}}\right)\tau_1 \tag{S37}$$

(note the factor in parentheses is always positive by assumption), then Eq. S35 has a unique solution for the remaining quantities:

$$\begin{aligned} \tau_3 &= \frac{\tau_2(h_{23} - h_{12}) - \tau_1(h_{13} - h_{12})}{h_{23} - h_{13}}, \\ \lambda_2 &= (\tau_1 - \tau_2)h_{12} + \lambda_1, \\ \lambda_3 &= (\tau_1 - \tau_2)\left(\frac{h_{23} - h_{12}}{h_{23} - h_{13}}\right)h_{13} + \lambda_1. \end{aligned} \tag{S38}$$

The linear system actually has a unique solution regardless of Eq. S37, but without that condition τ_3 may be negative. Therefore a set of three strains with unequal yields can all be pairwise conditionally-neutral only if the growth traits for strains 2 and 3 satisfy Eqs. S37 and S38. For example, one can construct three strains that all stably coexist in pairs in this manner.

We now turn to constructing sets of three strains such that there is a nontransitive cycle of selective advantage in binary competitions, i.e., strain 2 beats strain 1 in a binary competition, strain 3 beats strain 2, but strain 1 beats strain 3. Therefore the growth traits of the three strains must satisfy

$$\begin{aligned} (\tau_1 - \tau_2)h_{12} + \lambda_1 - \lambda_2 &> 0, \\ (\tau_2 - \tau_3)h_{23} + \lambda_2 - \lambda_3 &> 0, \\ (\tau_3 - \tau_1)h_{13} + \lambda_3 - \lambda_1 &> 0. \end{aligned} \tag{S39}$$

All three yields cannot be equal; if they are, adding together any two of the inequalities in Eq. S39 gives an inequality that is inconsistent with the third one. Otherwise, the three yields can take arbitrary values, including two of them being equal. Since we can cyclically permute the strain labels, without loss of generality we assume strain 1 has the smallest yield ($\nu_1 < \nu_2, \nu_3$). Therefore the harmonic mean logarithms obey $h_{23} > h_{12}, h_{13}$. We can also choose any values of τ_1 and λ_1 as before.

We must now choose the growth traits of strains 2 and 3 ($\tau_2, \tau_3, \lambda_2, \lambda_3$) to satisfy the inequalities of Eq. S39. We use a geometrical approach to understand the available region of trait space for these strains. The lag time for strain 3 is bounded from above and below according to (combining the second and third inequalities in Eq. S39)

$$(\tau_1 - \tau_3)h_{13} + \lambda_1 < \lambda_3 < (\tau_2 - \tau_3)h_{23} + \lambda_2. \tag{S40}$$

The upper and lower bounds are both functions of τ_3. The upper bound will be above the lower bound as long as τ_3 satisfies

$$\tau_3 < \frac{\tau_2 h_{23} - \tau_1 h_{13} + \lambda_2 - \lambda_1}{h_{23} - h_{13}}. \tag{S41}$$

Since τ_3 must be positive, this upper bound of τ_3 must also be positive. The denominator of the right-hand side of Eq. S41 is positive by assumptions about the yields, so therefore the numerator must be positive as well. This leads to a lower bound on the lag time of strain 2 λ_2; we can combine this with an upper bound on λ_2 from the first equation of Eq. S39 (strain 2 beats strain 1) to obtain

$$\tau_1 h_{13} - \tau_2 h_{23} + \lambda_1 < \lambda_2 < (\tau_1 - \tau_2)h_{12} + \lambda_1. \tag{S42}$$

Finally, the upper bound for λ_2 will be above the lower bound as long as τ_2 satisfies

$$\tau_2 > \max\left(\left(\frac{h_{13} - h_{12}}{h_{23} - h_{12}}\right)\tau_1, 0\right). \tag{S43}$$

Altogether, we can construct a set of nontransitive strains by choosing any yields ν_1, ν_2, ν_3 satisfying $\nu_1 < \nu_2, \nu_3$, and any values for the growth traits τ_1, λ_1 of strain 1; we then choose τ_2 according to Eq. S43 and λ_2 according to Eq. S42; finally, we choose τ_3 according to Eq. S41 and λ_3 according to Eq. S40.